September 2002 ECN-C--02-030

PERFORMANCE OF THE PV-SYSTEMS OF ECN BUILDING 31

N.J.C.M. van der Borg
M.J. Jansen

Acknowledgement/Preface

Principal:	European Commission
ECN project number:	7.4821.13.13
Principal's order number:	SE/00115/97/NL/DK
Programme:	THERMIE

Abstract

One of ECN's laboratory buildings was renovated using PV-systems. The power performance of all PV-systems was monitored on a daily basis (supervision monitoring) and of two selected systems the power performance was monitored in more detail (analytical monitoring).
The report presents the results of the first year of monitoring. The supervision monitoring revealed the failure of a serious number of inverters. With the analytical monitoring data a number of aspects, important for building integrated PV, were quantified. These aspects are:

- Thermal behaviour of the modules
- Loss of irradiation due to shading
- Additional energy loss due to partial shading (mismatch)
- Effect of dirt

Furthermore the irradiation data were used to validate the shading module of the design tool PVsyst. It was shown that PVsyst is a reliable tool for shading calculations.

CONTENTS

LIST OF TABLES

LIST OF FIGURES

SUMMARY

One of ECN's laboratory buildings was renovated using PV-systems. The power performance of all PV-systems was monitored on a daily basis (supervision monitoring) and of two selected systems the power performance was monitored in more detail (analytical monitoring).
The report presents the results of the first year of monitoring. The supervision monitoring revealed the failure of a serious number of inverters. With the analytical monitoring data a number of aspects, important for building integrated PV, were quantified. These aspects are:

- Thermal behaviour of the modules
- Loss of irradiation due to shading
- Additional energy loss due to partial shading (mismatch)
- Effect of dirt

Furthermore the irradiation data were used to validate the shading module of the design tool PVsyst. It was shown that PVsyst is a reliable tool for shading calculations.

1. INTRODUCTION

Building 31, Algemeen Lab (General Lab), is one of ECN's oldest buildings. It was built in 1963 and in 2001 a complete renovation took place. The renovation included the application of Photovoltaic Power systems on the roof and on sunshades in front of the South façade of the building. The realisation of the PV-systems was financially supported by the EU Thermie programme via the EC and by the Dutch NOZ-PV programme via NOVEM. A photo of the building with the PV-systems during construction is shown in figure 1.

All individual PV-systems are under daily surveillance (supervision monitoring) and two selected PV-systems are monitored intensively (analytical monitoring). The data are condensed into monthly data for sending overviews to JRC in Ispra, as part of the contractual obligations with the EC. The data are, of course, also used by ECN to evaluate the performance of the PV-systems in more detail. The results of this for the first monitoring year (8/8/2001 - 8/8/2002) are given in this report. The report gives a brief description of the PV-systems in chapter 2 and of the used monitoring system in chapter 3. The results of the supervision monitoring are given in chapter 4 and the results of the analytical monitoring in chapter 5.

More details on the architectural integration of the PV-systems into the building are given in reference [1]. Ongoing information on the performance of the PV-systems is available for all ECN-employees through the ECN-intranet (http://ecntsc/pvdaq4/).

Photo: Marcel van Kerckhoven. Copyrights: BEAR Architecten, Gouda NL.

Figure 1 *ECN building 31 and the various PV-systems under construction*

2. PV-SYSTEMS

2.1 Façade systems

The south façade of the building has sunshade devices made of lamellas at some distance in front of the façade and one awning above the upper lamellas that covers the spacing between the façade and the lamellas. The awning is semi-transparent because the applied PV-modules have a back cover made of glass and the spacing between the cells allows the passing of daylight.

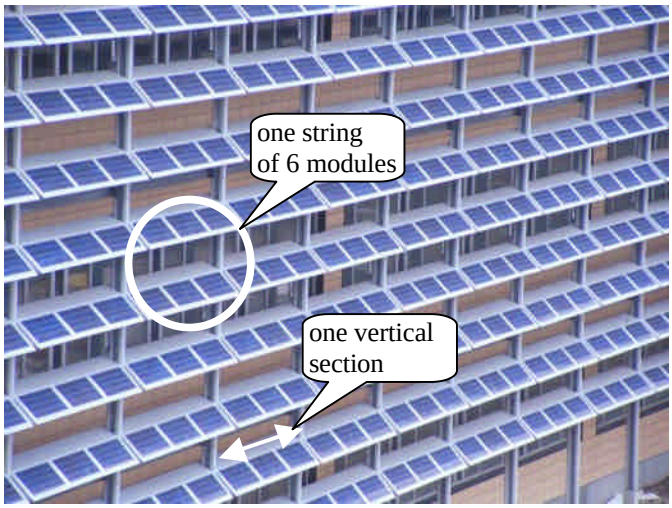

Photo: Marcel van Kerckhoven. Copyrights: BEAR Architecten, Gouda NL.

Figure 2 *Detail of the façade*

The PV-modules of the lamellas and of the awning are grouped into 13 vertical sections. Each section has a width of 3 modules (see figure 2) and a height of 14 lamellas. Since the 6 modules of two lamellas are connected into one string, totally 7 strings of 6 lamella modules are formed per vertical section. Also the modules of the awning are connected into strings of 6 modules. Each vertical section is completed with 2 strings of 6 awning modules. The 9 strings are connected in parallel on Sunmaster 2500 inverters made by Mastervolt.
Details of the façade systems are summarised in table 1.

Table 1 *Details of the façade systems*

Number of façade systems	13, all multi-crystalline silicon
Orientation of the façade	173• w.r.t. North
Number of inverters per system	1; Mastervolt Sunmaster 2500 (2500 W_{dc})
Number of façade strings per system	7; Tilt angle 38•
Number of awning strings per system	2; Tilt angle 18•
Number of façade modules per string	6; Shell Solar RSM 50 sb
Properties façade module	49 Wp @ 17.0 V; cell area 0.36 m^2 (36*0.01)
Number of awning modules per string	6; Shell Solar IRD 50
Properties awning module	44.4 Wp @ 16.6 V; cell area 0.36 m^2 (36*0.01)
Power per system	2590 Wp (7*6*49 + 2*6*44.4)
Total power of the façade systems	33.68 kWp (13*2590 Wp)

2.2 Roof systems

The roof systems follow the curvature of the roof of the building. The systems consist of 38 parallel strings with an azimuth angle of 173• w.r.t. North and a tilt angle of 6• (North side) to 14• (South side). Each string consists of 12 BP-Solarex 585-L modules (mono-crystalline silicon). Pairs of two strings are connected in parallel to SMA inverters, type BP Sunny Boy 2400 (nominal output power 1500 W).
Details of the roof systems are summarised in table 2.

Table 2 *Details of the roof systems*

Number of roof systems	19, all mono-crystalline silicon
Orientation of the façade	173• w.r.t. North
Number of inverters per system	1; BP Sunny Boy 2400 (1500 W_{ac})
Number of roof strings per system	2; Tilt angle from 6• to 14• (curved roof)
Number of roof modules per string	12; BP-Solarex 585-L 85
Properties roof module	85 Wp @ 18 V; cell area 0.53 m^2 (36*0.0147)
Power per system	2040 Wp (2*12*85)
Total power of the roof systems	38.76 kWp (19*2040 Wp)

3. MONITORING SYSTEM

3.1 General

The monitoring system is based on the LON-technology (Local Operating Network). The data acquisition is performed at several locations in the building using measurement instruments with LON-interfaces. The data are sent to a central PC through one digital data cable (data bus). The PC takes the initiative to measure the data for the supervision monitoring once per day and for the analytical monitoring about once per second. The raw data of the analytical monitoring are condensed into averaged values over 10-minute periods. These 10-minute data are stored, together with the daily data of the supervision monitoring, for subsequent offline evaluations. The measurement software (PVdaq4) was developed at ECN (unit TS&C).

3.2 Supervision monitoring system

For the purpose of supervision monitoring all 13 façade systems and all 19 roof systems are equipped with a kWh-counter with LON-interface. The readings are performed once per day, which results in daily energy production values for all individual PV-systems. Additionally 8 irradiance sensors are used, each of them connected to a digital integrator with LON-interface. These devices also result in daily readings of the total energy density of the irradiance, commonly called the daily irradiation. The devices for irradiance integration were developed and built at ECN (Unit TS&C). Details on the 8 irradiance sensors are given in table 3. The azimuth angle of all irradiance sensors is the same as of the PV-systems: 173•. A sketch of the position of the irradiance sensors is given in figure 3.

Table 3 *Details on the 8 irradiance sensors*

Name	Nr in fig. 3	Location (1)	Tilt angle	Type (4)	Additional information
H-hor	1	Roof 10 upper edge	0•	Pyranometer Kipp&Zn, CM21	(3)
H-roof high	2	Roof 10 upper edge	6•	Reference cell Shell Solar Energy	
H-roof low	3	Roof 10 lower edge	14•	Reference cell Shell Solar Energy	
H-awning	4	Awning 1 West edge	18•	Reference cell Shell Solar Energy	
H-lam1	5	Lamella 1 façade 7	38•	Reference module(2) Shell Solar Energy	Sensor failed
H-lam3	6	Lamella 3 façade 7	38•	Reference module(2) Shell Solar Energy	
H-lam5	7	Lamella 5 façade 7	38•	Reference module(2) Shell Solar Energy	
H-lam14	8	Lamella 14 façade 7	38•	Reference module(2) Shell Solar Energy	Sensor failed

(1) The PV-systems are numbered from West (façade system 1 and roof system 1) to East (façade system 13 and roof system 19). The lamellas are numbered from top (lamella 1) to bottom (lamella 14).

(2) A reference module is an adapted design of the lamella modules: 1 cell is disconnected from the rest and is used as a reference cell.

(3) During the monitoring programme the pyranometer data was judged as unreliable. Another pyranometer, of the same make and type, was mounted on 25 February 2002. Earlier data was obtained from a horizontally positioned pyranometer at another location at ECN (building 40).

(4) All reference cells and reference modules were made of multi-crystalline silicon. The reference cells and reference modules were calibrated in the ECN-laboratory (ref. [2]). The pyranometer was calibrated by its manufacturer.

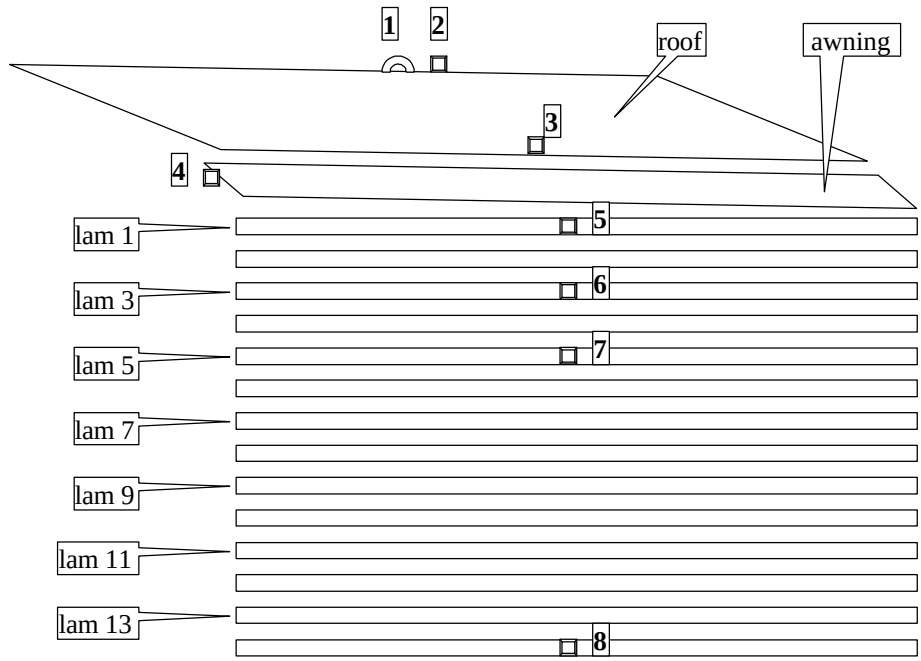

Figure 3 *Sketch of the position of the irradiance sensors. The numbers correspond to the numbers in table 3*

3.3 Analytical monitoring system

Two PV-systems were selected for the analytical monitoring programme: the central façade system (façade system number 7) and the central roof system (roof system number 10). Of both systems several quantities were measured such as irradiance, module temperature, array current, array voltage and, input power and output power of the inverter. Additionally the 9 string currents of the façade system were measured.
Details of the measured quantities are summarised in table 4.

Table 4 *Details of the measured quantities*

Name	description	sensor	additional information
G-hor	Horizontal global irradiance	pyranometer	see 2.3
T-amb	Ambient temperature	AD590	radiation shielded
G-lam1	In plane irradiance, lamella 1	Ref. module	see 2.3
G-lam3	In plane irradiance, lamella 3	Ref. module	see 2.3
G-lam5	In plane irradiance, lamella 5	Ref. module	see 2.3
G-lam14	In plane irradiance, lamella 14	Ref. module	see 2.3
G-roof high	In plane irradiance, roof high	Ref. cel	see 2.3
G-roof low	In plane irradiance, roof low	Ref. cel	see 2.3
G-awning	In plane irradiance, awning	Ref. cel	see 2.3
Tm-lam1	Module temperature, lamella 1	AD590	sensor laminated
Tm-lam3	Module temperature, lamella 3	AD590	sensor laminated
Tm-lam5	Module temperature, lamella 5	AD590	sensor laminated
Tm-lam14	Module temperature, lamella 14	AD590	sensor laminated
Tm-roof high	Module temperature, roof high	AD590	sensor glued at rear
Tm-roof low	Module temperature, roof low	AD590	sensor glued at rear
Tm-awning	Module temperature, awning	AD590	sensor glued at rear
Udc-façade7	Input voltage inverter façade 7	U-divider	
Udc-roof10	Input voltage inverter roof 10	U-divider	
Idc-façade7	Input current inverter façade 7	I-Shunt	
I7-string1	Current in façade 7 string 1	I-LEM	
I7-string2	Current in façade 7 string 2	I-LEM	
I7-string3	Current in façade 7 string 3	I-LEM	
I7-string4	Current in façade 7 string 4	I-LEM	
I7-string5	Current in façade 7 string 5	I-LEM	
I7-string6	Current in façade 7 string 6	I-LEM	
I7-string7	Current in façade 7 string 7	I-LEM	
I7-string8	Current in façade 7 string 8	I-LEM	
I7-string9	Current in façade 7 string 9	I-LEM	
Idc-roof10	Input current inverter roof 10	I-Shunt	
Pdc-façade7	Input power inverter façade 7	Analogue multiplication Idc * Udc	
Pdc-roof10	Input power inverter roof 10	Analogue multiplication Idc * Udc	
Pac-façade7	Output power inverter façade 7	I-shunt	Analogue Iac * Uac
Pac-roof10	Output power inverter roof 10	I-shunt	Analogue Iac * Uac

4. RESULTS SUPERVISION MONITORING

The supervision monitoring system (3.2) results in daily readings of the kWh-counters of all individual PV-systems and in daily readings of the irradiance integrators. The monthly energy production of the systems and the monthly irradiation values are calculated as the differences between these readings at the end and at the beginning of each month. The monthly performance ratio is calculated for each PV-system with the following formula.

$$PR = \frac{E}{P_{stc}} / \frac{H_i}{G_i}$$

with PR = monthly performance ratio (-)
E = monthly energy production of the PV-system (kWh)
P_{stc} = nominal power (2.04 kWp for roof, 2.59 kWp for façade system)
H_i = monthly in plane irradiation (kWh/m^2); see below
G_i = reference value for the in plane irradiance (1 kW/m^2)

The definition of the in plane irradiation values is not unambiguous for the roof systems (due to the curvature of the arrays) and also for the façade systems (due to the differences in tilt and shading of the awning and lamella modules). As an arbitrary choice the irradiation of the roof system is calculated as the average of the upper and lower edge of the roof and of the façade systems as the area-weighted average of the awning and of the lamellas (lamella 5).

$$H_i(roof) = (H\_roof_{high} + H\_roof_{low}) / 2$$
$$H_i(facade) = (7 * H\_lam5 + 2 * H\_awning) / 9$$

The performance ratios of the individual PV-systems are presented graphically in the figures 4 through 10.

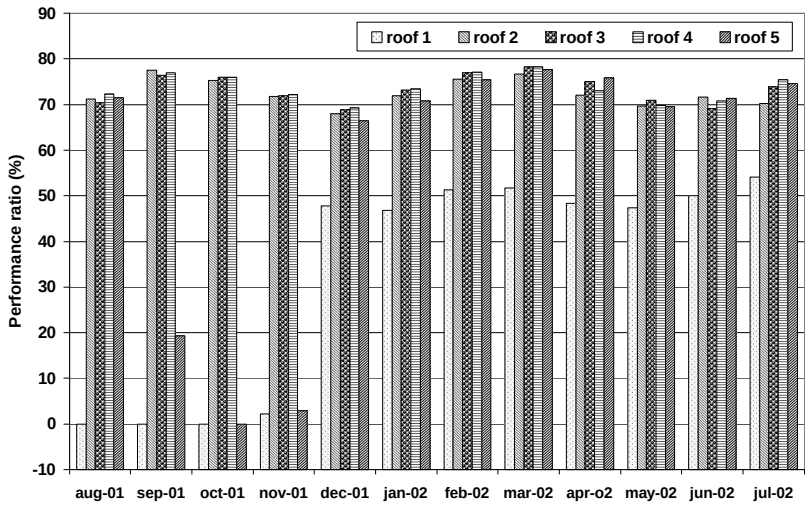

Figure 4 *Performance ratios of the roof systems 1 through 5*

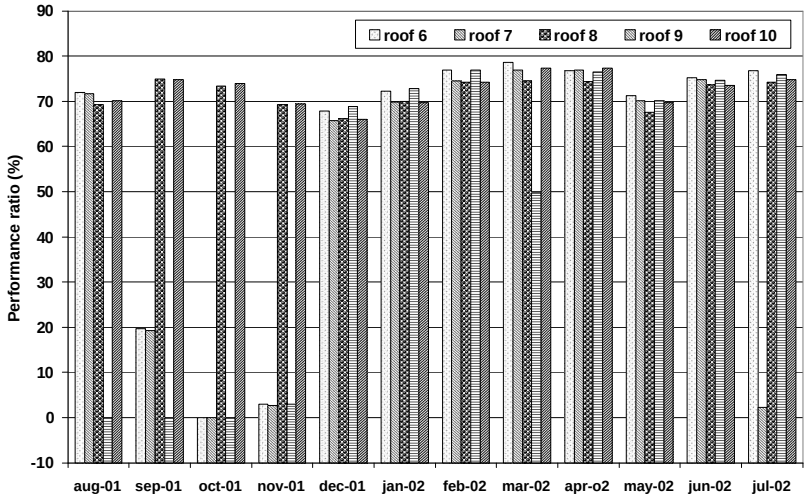

Figure 5 *Performance ratios of the roof systems 6 through 10*

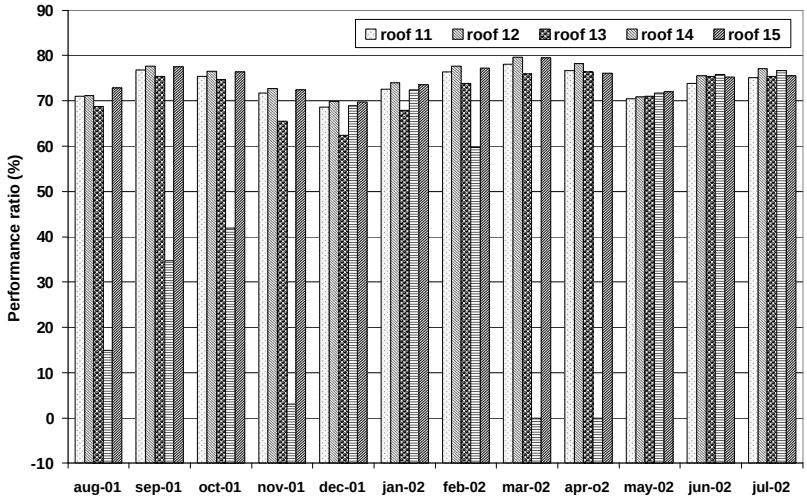

Figure 6 *Performance ratios of the roof systems 11 through 15*

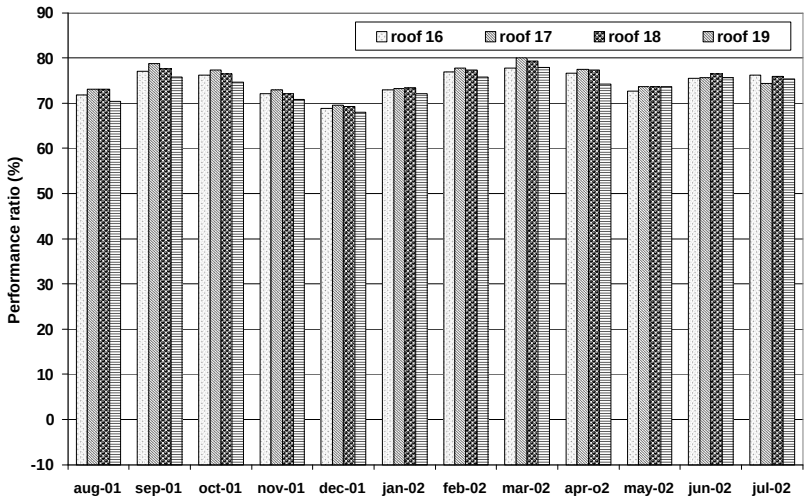

Figure 7 *Performance ratios of the roof systems 16 through 19*

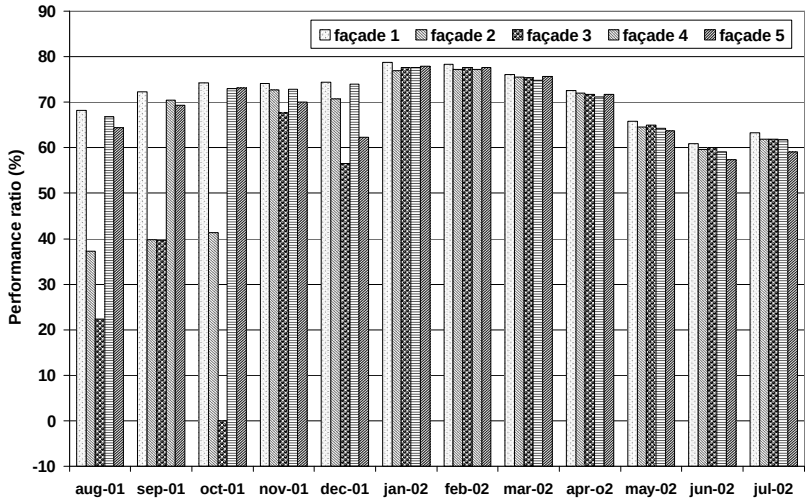

Figure 8 *Performance ratios of the façade systems 1 through 5*

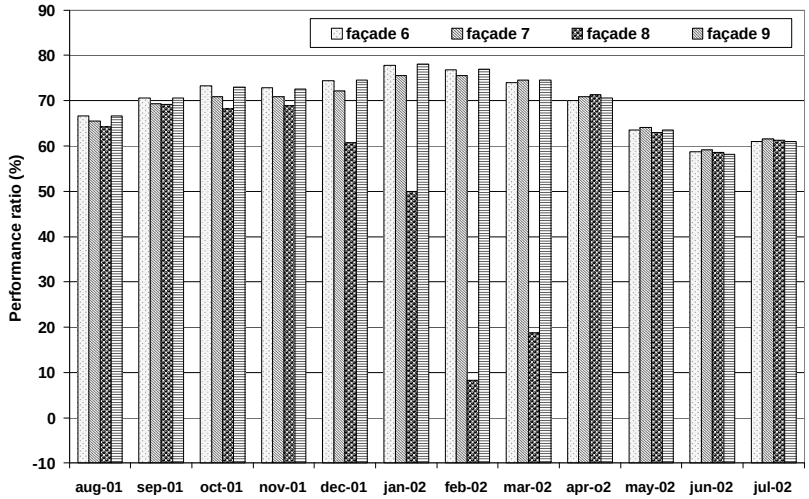

Figure 9 *Performance ratios of the façade systems 6 through 9*

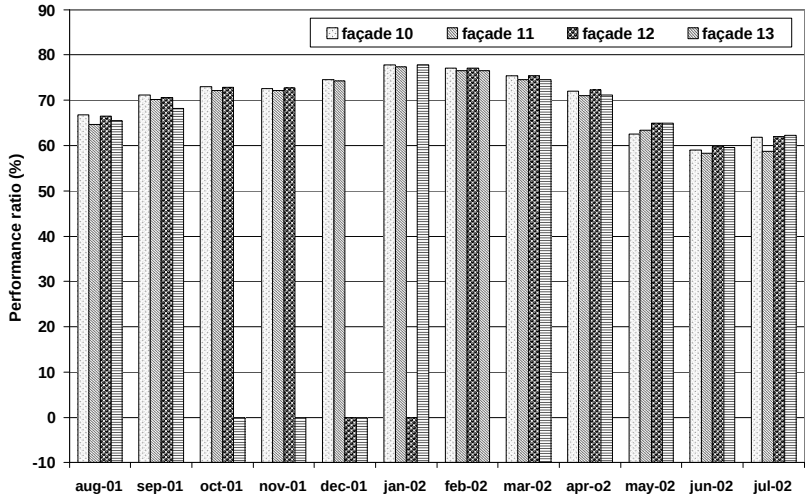

Figure 10 *Performance ratios of the façade systems 10 through 13*

The figures 4 through 10 show that not all PV-systems have performed properly during all months. This is caused by a number of failures, described below. Furthermore the inverter of roof system 14 was temporarily removed for inspection by BP from 5/3/02 - 23/4/02.
On the roof of the building a movable catwalk was constructed for accessing the roof modules. It is parked very close to roof system 1. Its shading is probably the cause of the lower performance of roof system 1 during all months.

Failing roof systems.
The AC-fuse of 6 roof systems failed several times. Examination of the systems showed that

- the systems switched off and on (very frequently) at high irradiance values and
- (very often) the inrush current had extemely high values.

The results of this research are described in reference [3]. The manufacturer of the inverters decided to solve this problem by implementing new software in the inverters on March 26th 2002. After this date the AC-fuses remained intact until roof system 7 blew its AC-fuse again on July 7th 2002.

Failing façade systems.
The inverters of 5 façade systems failed and had to be replaced by other inverters of the same type. The cause of the failures is unknown at ECN.

An overview of the PV-systems with low performance is given in table 5.

Table 5 *PV-systems with low performance*

PV-system	Reason
Roof 1	AC-fuse failures until 26/03/02 Shading by catwalk
Roof 5	AC-fuse failures until 26/03/02
Roof 6	AC-fuse failures until 26/03/02
Roof 7	AC-fuse failures until 26/03/02 AC-fuse failure at 3/7/02 (replaced at 7/8/02)
Roof 9	AC-fuse failures until 26/03/02
Roof 14	AC-fuse failures until 26/03/02 Inverter removed for inspection by BP from 5/3/02 - 23/4/02
Façade 2	Inverter failure (replaced on 14/12/01 by Shell Solar Energy)
Façade 3	Inverter failure (replaced on 14/12/01 by Shell Solar Energy)
Façade 8	Inverter failure (replaced on 26/3/02 by Shell Solar Energy)
Façade 12	Inverter failure (replaced on 25/01/02 by Shell Solar Energy)
Façade 13	Inverter failure (replaced on 14/12/01 by Shell Solar Energy)

The annual energy production of a normal operating roof system and of a normal operating façade system was determined from the reading of the kWh-counters of roof system 10 and façade system 7 on August 8th 2001 and August 8th 2002. Over the same period the irradiation values were measured with the irradiance sensors connected to the irradiance integrators. The resulting performance data are given in table 6.

Table 6 *Performance data of the two types of PV-systems*

	Roof system 10	Façade system 7
E (kWh) Annual energy production	1704	1868
Y (kWh/kWp) Annual yield	835	721
H_o (kWh/m^2) global irradiation on horizontal plane	1090	
H_i (kWh/m^2) Averaged in-plane irradiation	1137	1066
PR (%) Annual Performance ratio	73.5	67.7
Y_{1000} (kWh/kWp) Annual yield normalised to a standard year (ref.[4])	766	661

5. RESULTS ANALYTICAL MONITORING

5.1 Array efficiency

5.1.1 Roof system

The array efficiency of the PV-system was calculated for each of the 10-minutes period of the monitoring year. The efficiency is based on the effective area (the cell area) and it is corrected to a module temperature of 25 •C (using the temperature coefficient for the power of x-Si). Also the measured irradiance is corrected to a module temperature of 25 •C (using the temperature coefficient for the short circuit current of x-Si).

$$\eta^{25}_{array} = \frac{E_{dc}}{H_{ic} * A} * [(1-\beta) * (T_m - 25)]$$

$$H_{ic} = (H_{ic}low + H_{ic}high)/2$$

$$H_{ic}low = H_i low * [(1+\alpha)(T_m - 25)]$$

$$H_{ic}high = H_i high * [(1+\alpha)(T_m - 25)]$$

$$T_m = (T_m low + T_m high)/2$$

$$\alpha = 0.0007\ K^{-1}$$

$$\beta = -0.004\ K^{-1}$$

$$A = 12.7\ m^2$$

As can be seen in the formulas above, the irradiance is arbitrarily defined as the average of the irradiance at the upper edge and at the lower edge of the roof system. Due to the curvature of the roof the irradiance along the strings is not uniform, depending of the time of day, of the day of the year and of the sky conditions. It is expected that the array efficiency is smaller at non-uniform irradiance than at uniform irradiance because of the mismatch effect. This is illustrated in figure 11 where the array efficiency is plotted against the irradiance. It shows three graphs:

- All data points of the year
- Only data points with uniform irradiation ($0.98 < H_{\text{upper/lower edge}} < 1.02$)
- Only data points with non-uniform irradiation ($0.78 < H_{\text{upper/lower edge}} < 0.82$)

The data points of the graphs have been sorted and averaged in irradiance bins with a width of 20 W/m^2 before plotting them in the figure.

Comparison of the graphs in figure 11 for uniform and non-uniform irradiance shows that, indeed, the mismatch effect is strong under non-uniform irradiance. However on an annual basis, using all data points, the efficiency curve is very close to the curve for uniform iradiance. In fact it is about a factor 0.98 lower. From this it is concluded that the curvature of the roof causes a mismatch loss on annual basis of only about 2%.

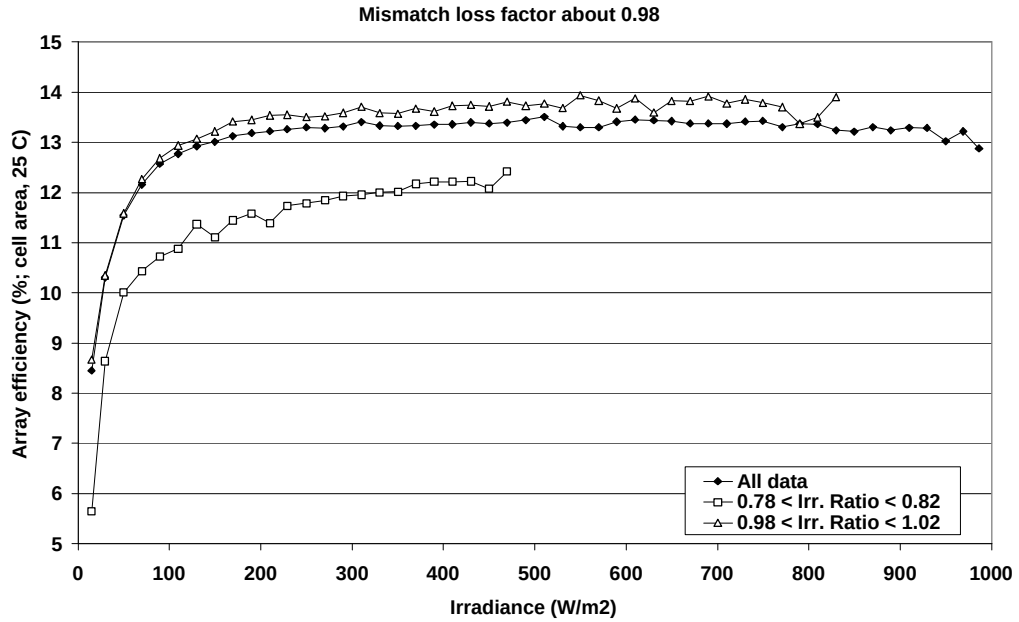

Figure 11 *Efficiency of the roof array with the ratio between the irradiance at the upper edge and at the lower edge of the roof as a parameter*

5.1.2 Façade system

The array efficiency of the PV-system is calculated for each of the 10-minutes period of the monitoring year similarly to the roof system (5.1.1).

$$\eta^{25}_{array} = \frac{E_{dc}}{H_{ic} * A} * [(1-\beta) * (T_m - 25)]$$

$$H_{ic} = (7 * H_{ic}lam5 + 2 * H_{ic}awning)/9$$

$$H_{ic}lam5 = H_i lam5 * [(1+\alpha)(T_m - 25)]$$

$$H_{ic}awning = H_i awning * [(1+\alpha)(T_m - 25)]$$

$$T_m = (7 * T_m lam5 + 2 * T_m awning)/9$$

$$\alpha = 0.0007 \ K^{-1}$$

$$\beta = -0.004 \ K^{-1}$$

$$A = 19.44 \ m^2$$

As can be seen in the formulas the irradiance is arbitrarily defined as the area-weighted average of the irradiance at the awning and at lamella 5. The irradiance at lamella 5 is considered to be representative for all lamellas, even for the upper one (above lamella 1 a metal rim was constructed which acts as a "dummy lamella 0"). It is not expected that differences between the irradiance on the awning and on the lamellas cause a significant mismatch effect because the regarded strings are connected in parallel, not in series. In the summer months however the lamella modules are partly shaded, depending of the time of the day and of the sky conditions. The reference cells of the lamellas are integrated in the modules. Therefore the measured irradiance is considered as a representative irradiance for the entire module. At moments of partial shading a mismatch effect will occur within the string of 36 cells of each module. This is

illustrated in figure 12 where the array efficiency is plotted against the irradiance. It shows three graphs:

- All data points of the year
- Only the data points of March 2002 (no partial shading expected)
- Only the data points of June 2002 (moments of partial shading expected)

The data points of the graphs have been sorted and averaged in irradiance bins with a width of 20 W/m^2 before plotting them in the figure.

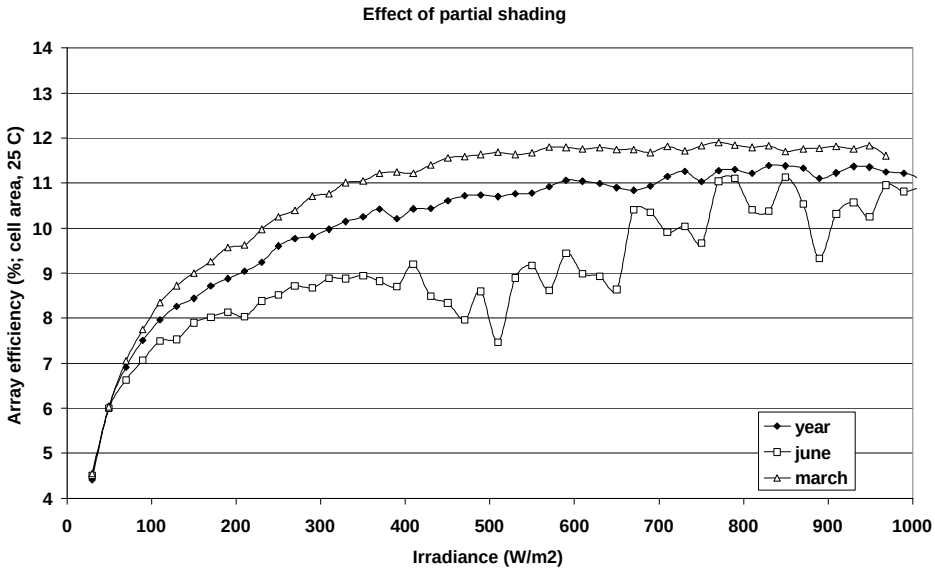

Figure 12 *Array efficiency of the façade system*

The curve in figure 12 for June shows indeed lower values for the efficiency. Comparing the curve for the whole year with the curve of March shows that the loss factor due to partial shading of the lamellas is about 0.94 on an annual basis for the complete array (including the awning strings).

5.2 Inverter efficiency

The conversion efficiency of both inverters was calculated by dividing the output energy by the input energy of each of the 10-minutes period of the year. This resulted in data pairs of input power and conversion efficiency. The data pairs were sorted and averaged in power bins with a width of 20 W. The resulting efficiency curves are given in figure 13.

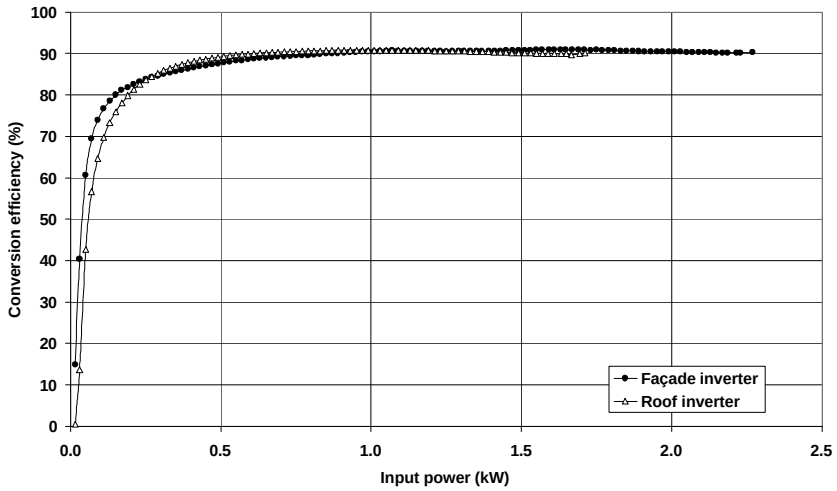

Figure 13 *Conversion efficiency of the two applied inverters*

5.3 Module temperature

The difference between the temperatures of the module and the ambient temperature were calculated for all 10-minutes periods of the year. The data were sorted and averaged in irradiance bins with a width of 20 W/m^2 . The results are given in the figures 14 (lamellas), 15 (awning) and 16 (roof).

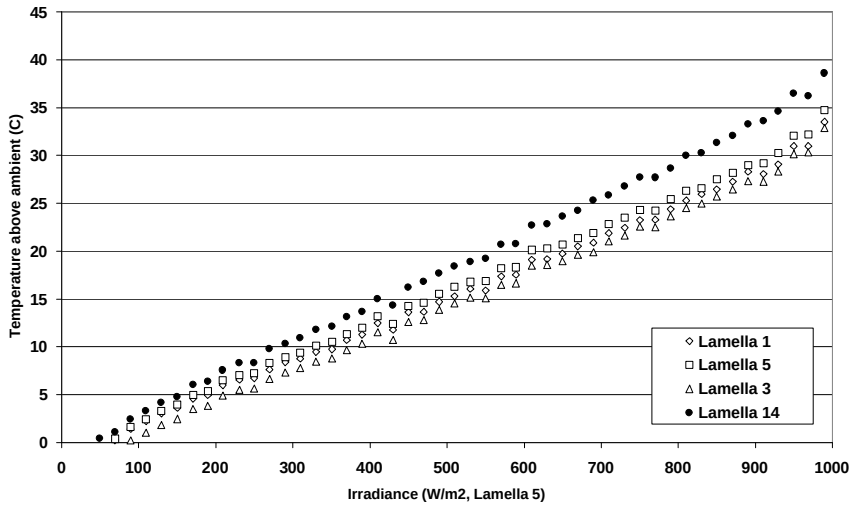

Figure 14 *Difference between the temperatures of the lamella modules and the ambient temperature*

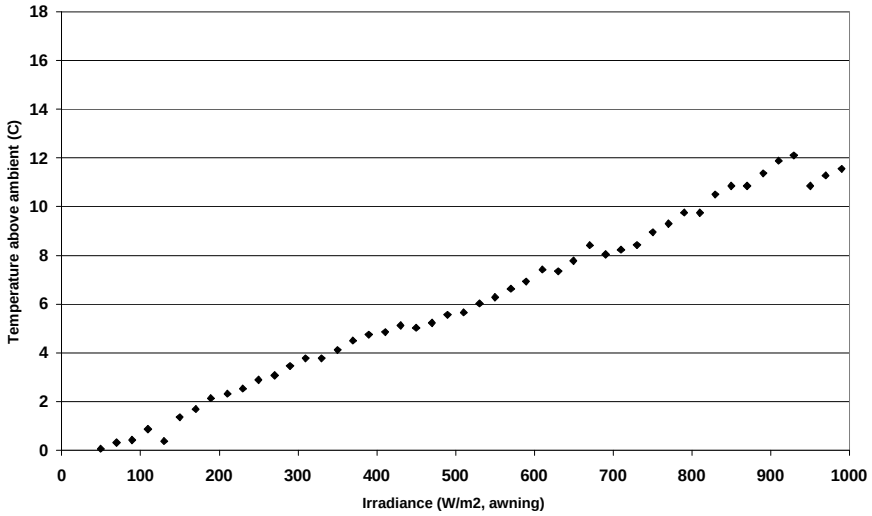

Figure 15 *Difference between the temperatures of the awning modules and the ambient temperature*

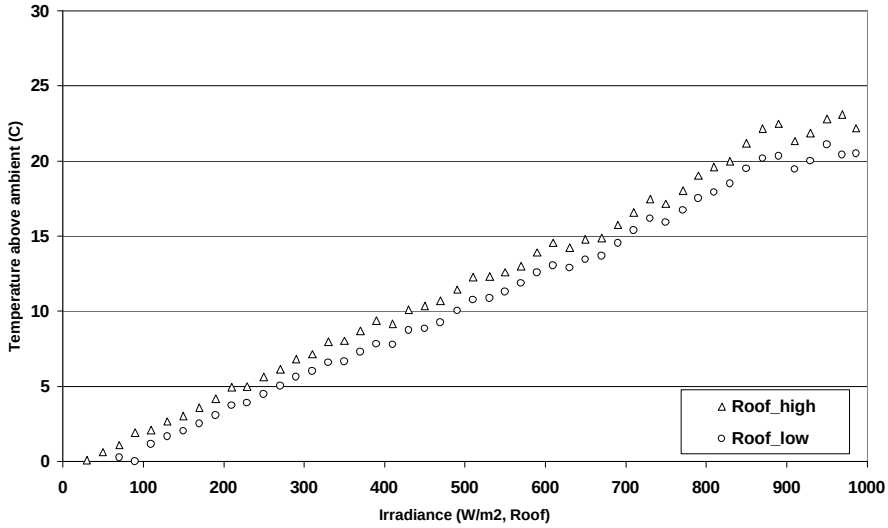

Figure 16 *Difference between the temperatures of the roof modules and the ambient temperature*

The figures show that the raise of the module temperature above the ambient temperature is highest for the lamellas (about 35 •C at 1000 W/m^2) and lowest for the awning (about 12 •C at 1000 W/m^2). For the roof modules the temperature raise is about 23 •C at 1000 W/m^2. These differences in temperatures of the three groups of modules are caused by differences in the absorption coefficient of the three module types and, probably much more important, differences in the ventilation. This is shown in the photos of the three groups of modules in the figures 17, 18 and 19. The lamella modules are positioned on a box-shape structure with small ventilation holes near the lower edge (visible in figure 17) and near the upper edge (not visible in figure 17). The awning modules are of the see-through type and have no cover underneath. The roof lamellas have a ventilation space between the roof and the support structure of 4 cm and between the roof and the modules of 8 cm.

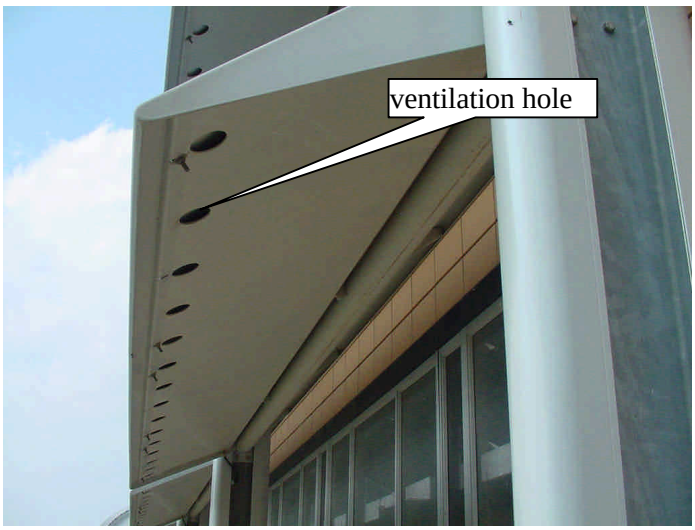

Figure 17 *Photo of the support structure of the lamella modules*


Figure 18 *Photo of the support structure of the awning modules*

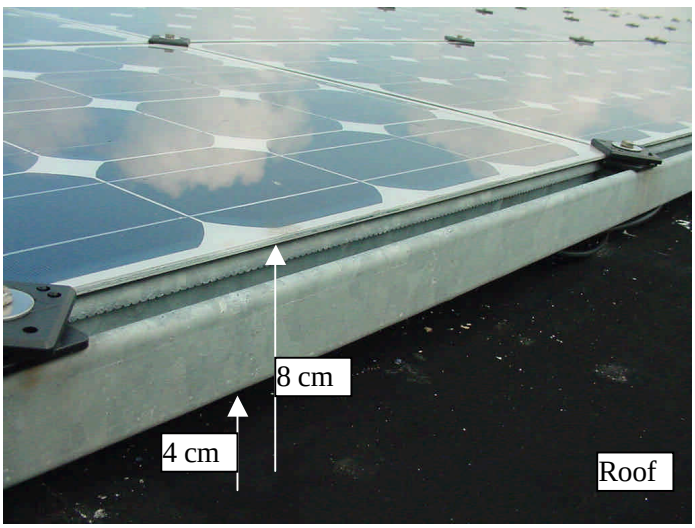

Figure 19 *Photo of the support structure of the roof modules*

5.4 Effect of dirt

5.4.1 General

The PV-modules were never cleaned since the installation otherwise than the natural cleaning by rain. To obtain a rough estimation of the annual energy loss due to the dirt accumulation on the modules a kind of "snap shot experiment" was performed for the roof systems and also for the façade systems. Both experiments were performed at the end of the first monitoring year using the data obtained with the supervision monitoring system (paragraph 3.2).

5.4.2 Roof systems

A movable catwalk on the roof gives access to the roof systems. Via this catwalk both strings of one of the systems (number 3) were cleaned using water and sponge on July 19th 2002 while the other strings remained dirty. The dirt on the modules consisted mainly of excrements of birds (sea gulls). An impression of the energy loss due to the dirt was obtained by comparing the daily energy production of the cleaned system (number 3) with that of its dirty neighbouring system (number 4), both before and after the cleaning. The ratio of these daily energy productions is given in figure 20.

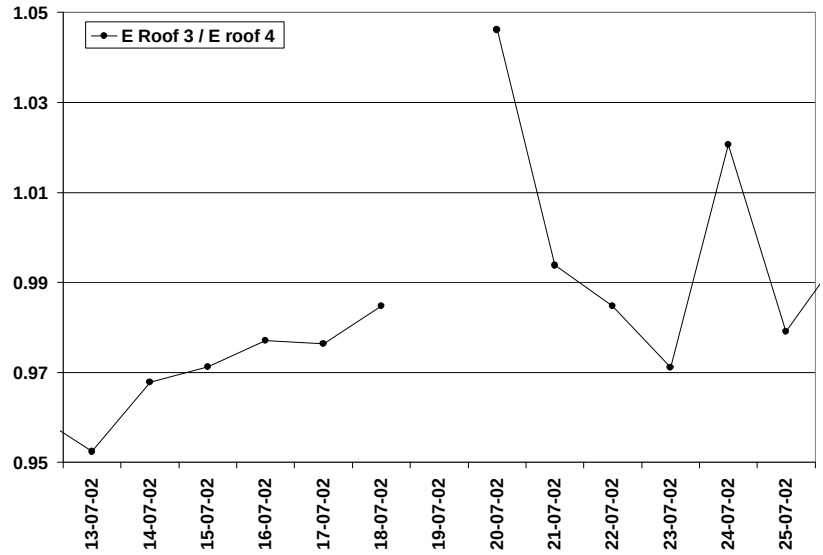

Figure 20 *Ratio of the daily energy production of roof system 3 and 4 (3 was cleaned at 19/07/02)*

The figure shows that the cleaning resulted in an increase of the energy production of about 5% on the first day after the cleaning. However this increase disappeared in a few days which indicates that the equilibrium between dirt production and natural washing settles in only a few days.

5.4.3 Lamella modules

Fixed catwalks are present against the façade behind the lamellas. Via these catwalk one of the reference modules (of lamella 3) was cleaned using water and sponge on August 2nd 2002 while the other modules remained dirty. In contrast to the roof modules no bird excrements were visible on the lamella modules. The dirt on the modules consisted of a thin layer of fouling. An impression of the irradiation loss due to the dirt was obtained by comparing the daily irradiation of the cleaned reference module (number 3) with that of the dirty neighbouring reference module (number 5), both before and after the cleaning. The ratio of these daily irradiations is given in figure 21.

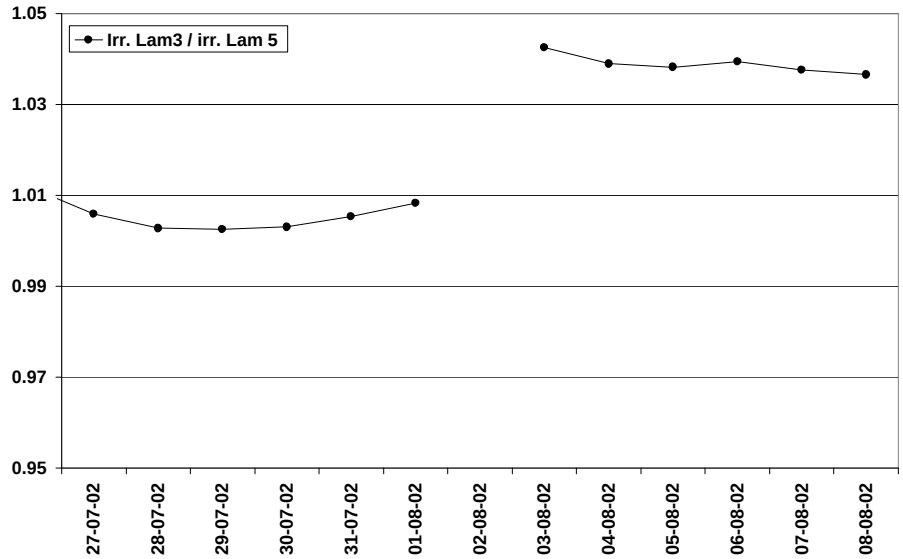

Figure 21 *Ratio of the daily irradiation on lamella 3 and 5 (3 was cleaned at 2/8/2002)*

The figure shows that the cleaning resulted in an increase of the irradiation of about 4% on the first day after the cleaning. This increase does not disappear in the first week, which indicates that the equilibrium between dirt production and natural washing settles slowly.

5.5 Effect of shading

5.5.1 General

The lamellas were designed as sunshade devices and as support structures for the PV-modules. As a consequence of combining both functions, the modules on the lamellas are shaded by the above placed lamellas during certain periods of the year. This is also the case for the upper lamella because of the metal rim above it which acts as a "dummy lamella 0". The shading includes the obstruction of direct radiation from the sun but also the obstruction of diffuse irradiance from the sky. The amount of shading depends on the time of the day, the day of the year and the sky conditions.
The effect of shading is twofold:

- loss of potential irradiance on the modules and
- loss of performance due to the mismatch effect in case of non-homogeneous irradiance within a string of cells or modules.

The effect of mismatch has been elaborated in the paragraphs 5.1.1 (roof) and 5.1.2 (façade). The loss of potential irradiance on the modules is addressed in this paragraph.

The loss of irradiance on the lamellas due to the shading was not measured but quantified by simulations (paragraph 5.5.3). The used simulation tool (PVsyst V3.12) was validated first (paragraph 5.5.2) using the measured data.

5.5.2 Validation of PVsyst

The building 31 and some of the neighbouring buildings were modelled using the facilities of PVsyst. The curved roof is simplified by the use of two flat planes. The model is given below.

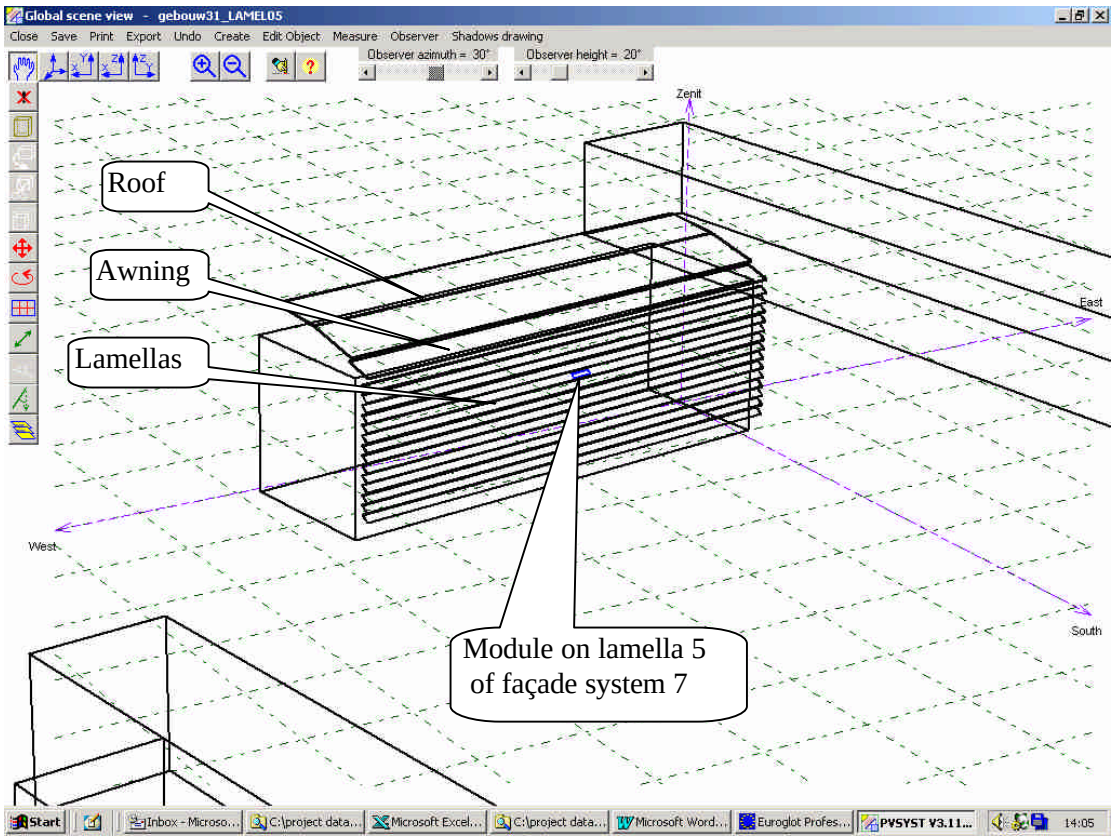

Figure 22 *The shading model applied in PVsyst*

The averaged values of the irradiance sensors of the 10-minutes periods were condensed into hourly irradiation values for the period from 8/8/2001 to 8/8/2002. The results were used to make a data set for a complete year from January 1st to December 31st. The global irradiation on the horizontal plane, measured with the pyranometer, was given as input to PVsyst. With these values PVsyst calculated the diffuse component of the global irradiation on the horizontal plane using the Liu & Jordans correlation. With these data PVsyst calculated the in plane irradiation using the Perez model. The shading calculations were performed with the "near shading option" of PVsyst. The ground reflection coefficient (albedo) was set to 0.20. The reflection loss on the surface of the modules, and thus on the surface of the reference cells, was accounted for using the ASHRAE-model (bo = 0.05). More details on PVsyst can be found at http://www.unige.ch/cuepe/pvsyst/pvsyst/index.htm.

With PVsyst the irradiation on the following positions were calculated:

- Upper edge of the roof, without shading obstacles
- Lower edge of the roof, without shading obstacles
- Awning, without shading obstacles
- Central module of lamella 5, with shading obstacles

The hourly values were summed into monthly irradiation values. The results of the simulated data and the measured data are given in the figures 23 through 26.

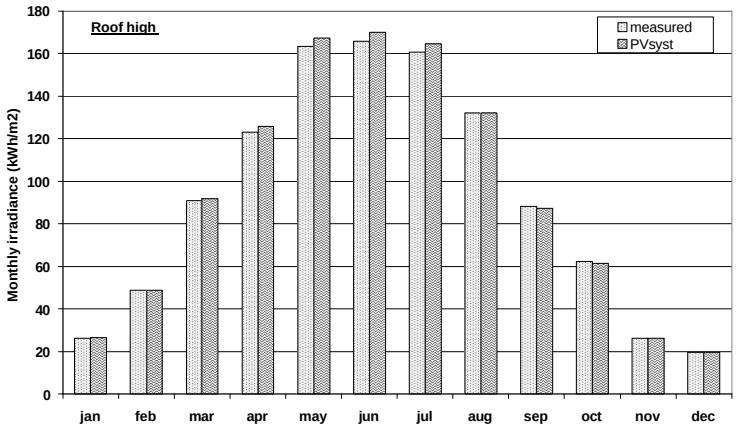

Figure 23 *Measured and simulated monthly irradiance values on the upper edge of the roof systems*

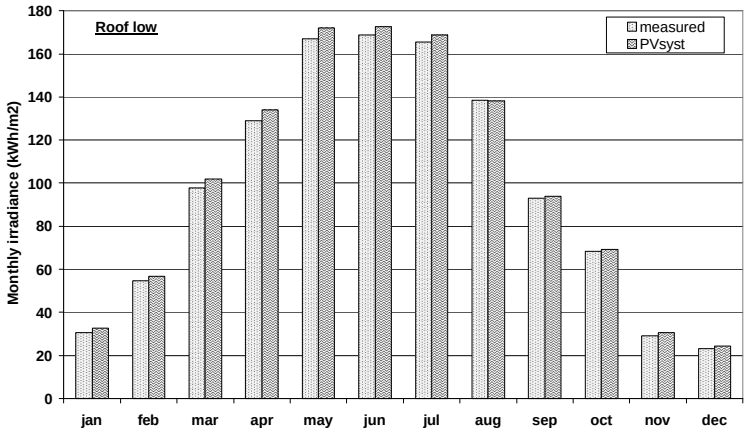

Figure 24 *Measured and simulated monthly irradiance values on the lower edge of the roof systems*

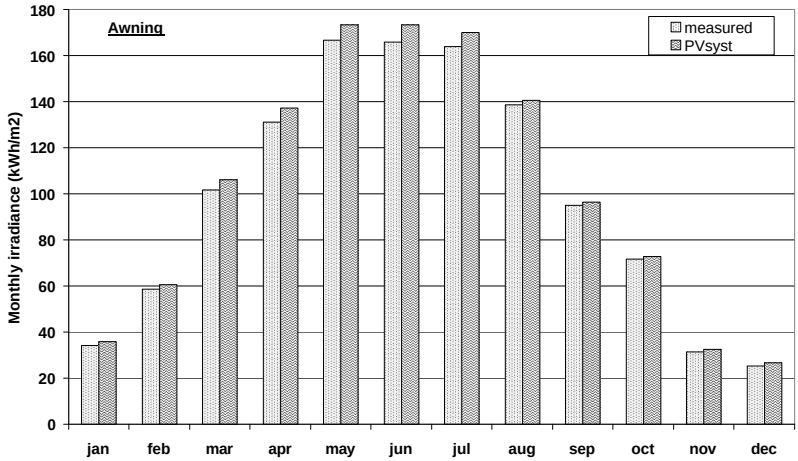

Figure 25 *Measured and simulated monthly irradiance values on the awning*

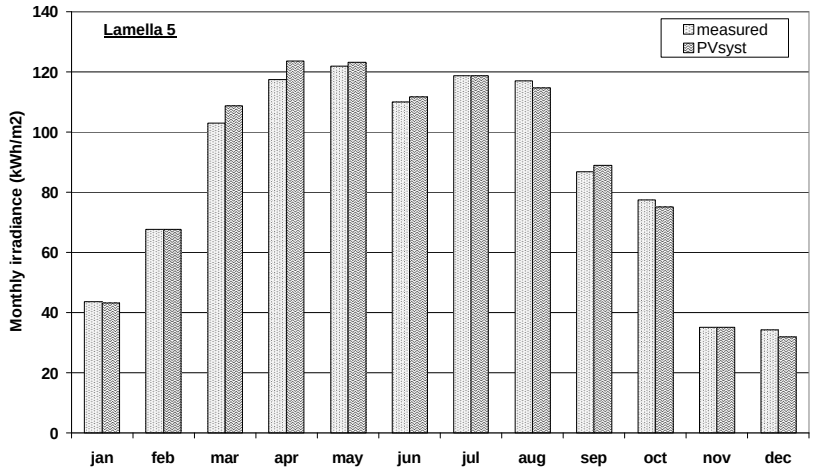

Figure 26 *Measured and simulated monthly irradiance values on lamella 5*

The figures show a very good correspondence between the measured and simulated monthly irradiation values. From this it was concluded that the loss of irradiance due to shading could reliably be calculated with PVsyst.

5.5.3 Irradiance loss

The loss of irradiance due to shading was calculated with PVsyst in a similar way as described in 5.5.2. The calculations were performed for the following situations:

- Central module of lamella 5, with shading obstacles (lamellas, building 31 and neighbouring buildings)
- Central module of lamella 5, with shading obstacles except the neighbouring buildings
- Central module of lamella 5, without any shading obstacle

The irradiation loss factor due to shading was calculated by dividing the monthly irradiation values calculated with the shading obstacles and calculated without the shading obstacles. From the results it was concluded that the neighbouring buildings did not cause any shading effect. The calculations were repeated for the central module of the lowest lamella (lamella 14). For this lamella it was shown that the effect of the neighbouring buildings on the annual irradiation was a factor of 0.98.

The results of the simulated shading on the central module of lamella 5 are given in figure 27.

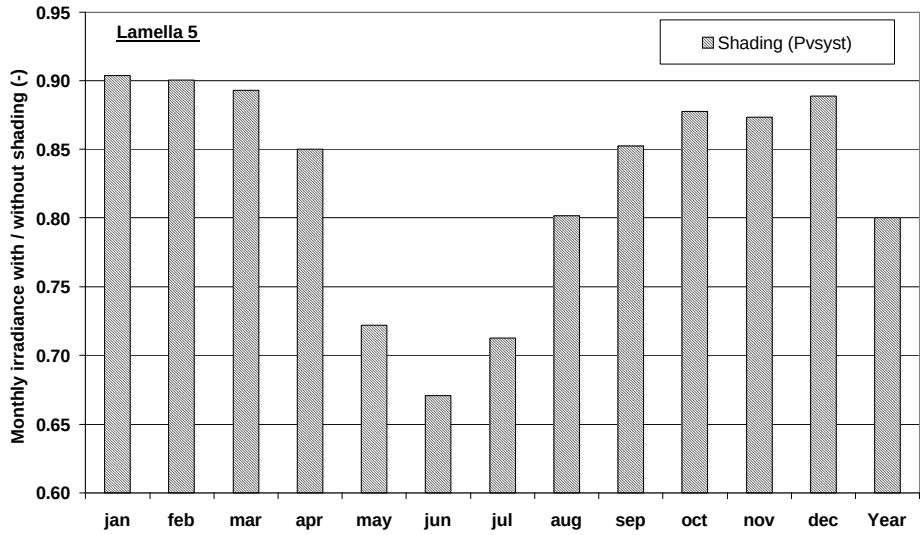

Figure 27 *Simulated monthly shading factor on lamella 5*

The figure shows that the shading effect of the building and the lamellas on the irradiation on the central module of lamella 5 is, of course, dependent on the month and that the annual irradiation loss factor is 0.80.

5.6 Performance of the individual façade strings

The contribution of the various strings of the façade system to the total production of the system can be shown using the currents of the various strings since their voltages are identical. The currents have been summed into monthly Ah-values for each of the 9 strings of façade system 7. The results are given in figure 28.

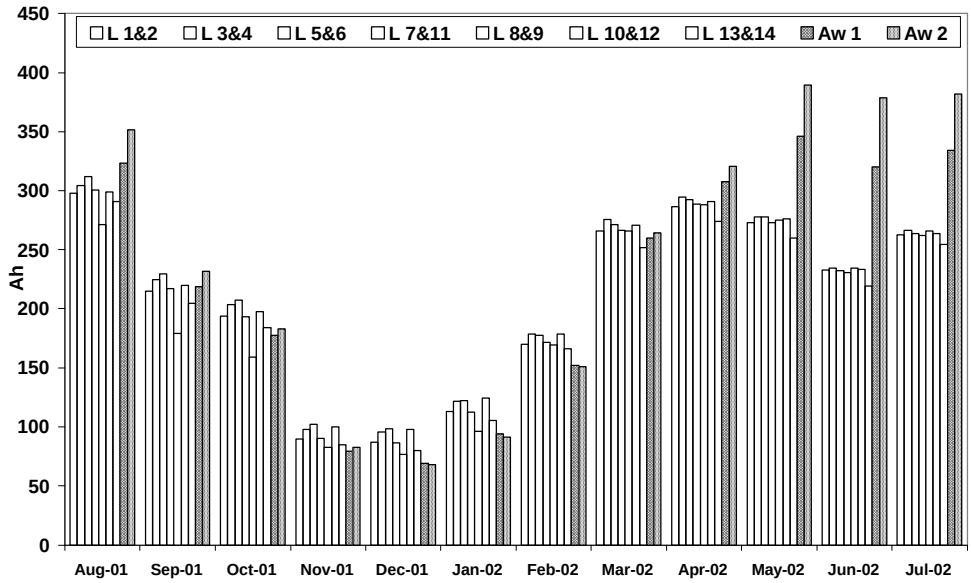

Figure 28 *Monthly Ah-values for each of the 9 strings of façade system 7*

The figure shows the following.

- The performance of string "Lam8 & Lam9" is lower than its neighbouring strings until February 2002. This was caused by one failing module in the string. The module was replaced by Shell Solar Energy on February 8th 2002.
- The performance of string "Lam13 & Lam 14" is always lower than its neighbouring lamella strings. On annual basis the difference is about 5%. This is partly accounted for by the shading effect of the neighbouring buildings (estimated at 2%; paragraph 5.5.3) and the somewhat higher module temperature (maximum 5ºC, estimated loss 2%).
- The performance of the awning strings differs very much from the lamella strings. This is obviously mainly caused by the differences in the orientation and in the shading effect.
- The performance of string "Awning 1" is lower than of string "Awning 2" in the summer period. This is probably caused by the shading effect of the lower rim of the roof that protrudes somewhat above the first row of awning modules. It affects more modules of Awning 1 than of Awning 2, as depicted in the following sketch of the layout of the modules.

Lower rim of the roof (North of awning)		
Awning 1	Awning 1	Awning 2
Awning 1	Awning 1	Awning 2
Awning 1	Awning 2	Awning 2
Awning 1	Awning 2	Awning 2

Figure 29 *Sketch of the module layout of the two awning strings of each façade system*

6. CONCLUSIONS

The supervision monitoring programme resulted in the following conclusions.

- The inverters of six roof systems failed once or more. This amounts to 31% of the total number of roof inverters.
- The inverters of five façade systems failed once. This amounts to 38% of the total number of facade inverters.
- The normalised annual yield of well functioning systems is 766 kWh/kWp for the roof systems and 661 kWh/kWp for the façade systems. These values reflect not only the quality of the PV-systems but also the available irradiation on the arrays. The two types of PV-systems have differences in the available irradiation due to the differences in the orientation. Furthermore the façade systems have an annual irradiation loss factor of 0.8 due to shading (see analytical monitoring).
- The annual performance ratio of well functioning systems is 74% for the roof systems and 68% for the façade systems. If no mismatch loss would be caused by the roof curvature and by the partial shading of the lamellas (see analytical monitoring), these values would be 75% for the roof systems and 72% for the façade systems.

The analytical monitoring programme of the two selected PV-systems resulted in the following conclusions.

- The annual mismatch loss of the roof system due to the curvature of the strings amounts to a factor 0.98.
- The annual mismatch loss of the façade system due to the (sporadic) partial shading of the modules is estimated at a factor 0.94.
- The annual irradiation loss on the lamellas due to the shading by the building 31 and by the other lamellas amount to a factor 0.80. The shading loss due to the neighbouring buildings can be neglected.
- The simulation programme PVsyst (V3.12) is a reliable tool for the calculation of irradiation on a tilted plane, even in the presence of shading obstacles.
- The performance loss due to dirt on the roof systems is roughly estimated at 5%, however cleaning seems to have only temporarily effect. The performance loss due to dirt on the façade systems is roughly estimated at 4%, cleaning seems to have a significantly longer effect.
- The temperature rise of the modules above ambient temperature is high for the lamella modules (35ºC at 1000 W/m^2), medium for the roof modules (23ºC at 1000 W/m^2) and low for the awning modules (12ºC at 1000 W/m^2).

7. REFERENCES

[1] H.F. Kaan (ECN) and T.H. Reijenga (BEAR Architects): "Reftrofit & architectural integration of PV modules in façade and roof of an office & laboratory building, Petten"; ECN-C-02-039, April 2002.

[2] Personal communication with Henk Rieffe, ECN

[3] M.J. Jansen: "Investigations on a BP/SMA 2400 PV inverter";
ECN-Zon Memo-01-033

[4] NOVEM: "Recommended practices for the monitoring of grid connected PV-systems in the Netherlands" (in Dutch); RC 4154, February 1997